Experimental Neurology 379 (2024) 114851

Contents lists available at ScienceDirect

Experimental Neurology

journal homepage: www.elsevier.com/locate/yexnr

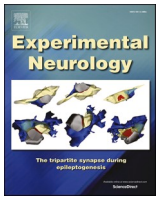

Research paper

Longitudinal quantitative assessment of TMEV-IDD-induced MS phenotypes in two inbred mouse strains using automated video tracking technology

Iskra Djabirska [a,b], Laetitia Delaval [a,b], Audrey Tromme [a,b], Joël Blomet [b], Daniel Desmecht [a], Anne-Sophie Van Laere [a,b,*]

[a] Department of Pathology, Fundamental and Applied Research for Animals & Health (FARAH), Faculty of Veterinary Medicine, University of Liege, Liège 4000, Belgium
[b] Prevor Research Laboratories, Valmondois 95760, France

ARTICLE INFO

Keywords:
TMEV-IDD
Multiple sclerosis
PhenoTyper
Spontaneous activity
Gait
Behavior

ABSTRACT

Multiple sclerosis (MS) is a chronic disabling disease of the central nervous system affecting over 2.5 million people worldwide. Theiler's murine encephalomyelitis virus-induced demyelinating disease (TMEV-IDD) is a murine model that reproduces the progressive form of MS and serves as a reference model for studying virus-induced demyelination.

Certain mouse strains such as SJL are highly susceptible to this virus and serve as a prototype strain for studying TMEV infection. Other strains such as SWR are also susceptible, but their disease course following TMEV infection differs from SJL's.

The quantification of motor and behavioral deficits following the induction of TMEV-IDD could help identify the differences between the two strains. Motor deficits have commonly been measured with the rotarod apparatus, but a multicomponent assessment tool has so far been lacking.

For that purpose, we present a novel way of quantifying locomotor deficits, gait alterations and behavioral changes in this well-established mouse model of multiple sclerosis by employing automated video analysis technology (The PhenoTyper, Noldus Information Technology). We followed 12 SJL and 12 SWR female mice and their mock-infected counterparts over a period of 9 months following TMEV-IDD induction.

We demonstrated that SJL and SWR mice both suffer significant gait alterations and reduced exploration following TMEV infection. However, SJL mice also display an earlier and more severe decline in spontaneous locomotion, especially in velocity, as well as in overall activity. Maintenance behaviors such as eating and grooming are not affected in either of the two strains. The system also showed differences in mock-infected mice from both strains, highlighting an age-related decline in spontaneous locomotion in the SJL strain, as opposed to hyperactivity in the SWR strain.

Our study confirms that this automated video tracking system can reliably track the progression of TMEV-IDD for 9 months. We have also shown how this system can be utilized for longitudinal phenotyping in mice by describing useful parameters that quantify locomotion, gait and behavior.

1. Introduction

Multiple sclerosis (MS) is a chronic inflammatory demyelinating disease of the central nervous system affecting over 2.5 million people worldwide. It remains the leading cause of non-traumatic neurological disability in young adults (Kingwell et al., 2013; Milo and Kahana,

Abbreviations: MS, multiple sclerosis; TMEV-IDD, Theiler's murine encephalomyelitis virus-induced demyelinating disease; EAE, experimental autoimmune/allergic encephalomyelitis; pi, post-infection; dpi, days post-infection; pfu, plaque-forming units; HLVs, horizontal locomotion values; ^{v}SJLs, virus-infected SJLs; ^{m}SJLs, mock-infected SJLs; ^{v}SWRs, virus-infected SWRs; ^{m}SWRs, mock-infected SWRs; DC, distance covered; WV, walking velocity; WF, walking frequency; VLVs, vertical locomotion values; URF, unsupported rearing frequency; TRV, total rearing velocity; GAs, gait alterations; TACP, turn angle of the center point; TATP, turn angle of tail base point; TCR, ratio of distance covered by tail base point and center point; EF, eating frequency; GF, grooming frequency; SRF, supported rearing frequency; SF, sniffing frequency; RD, resting duration.

* Corresponding author at: Department of Pathology, Fundamental and Applied Research for Animals & Health (FARAH), Faculty of Veterinary Medicine, University of Liege, Liège 4000, Belgium.

E-mail address: as.vanlaere@uliege.be (A.-S. Van Laere).

https://doi.org/10.1016/j.expneurol.2024.114851
Received 21 March 2024; Received in revised form 29 May 2024; Accepted 6 June 2024
Available online 13 June 2024

2010). The etiology of the disease, speculated to be multifactorial, is still undefined, which makes the development of effective therapeutic agents complicated. Mouse models have been invaluable tools in studying many human neurodegenerative diseases. In this regard, some of the most utilized models for studying different aspects of MS are the experimental autoimmune encephalomyelitis (EAE) model, Theiler's murine encephalomyelitis virus (TMEV)-induced demyelinating disease (TMEV-IDD) model and toxin-induced models of demyelination such as the cuprizone model (Denic et al., 2011; Procaccini et al., 2015).

TMEV-IDD in mice reproduces the acute or chronic *progressive* form of MS and represents a reference model of virus-induced demyelination. TMEV is a single-stranded RNA virus from the Picornaviridae family that was discovered by Max Theiler in 1934 (Oleszak et al., 2004).

Induction of the disease is achieved by direct intracerebral infection and the disease course and progression depend on the virulence of the viral strain as well as the mouse background. Typically, when subjects are injected with the DA strain of TMEV, the disease course is biphasic. The first (acute) phase is characterized by the apoptosis of neurons in gray and white matter a week after the inoculation, which clears within three weeks. Clinical manifestations are not common during the initial phase. The second phase starts about 1 month after infection, and its main hallmarks are chronic inflammation and demyelination with oligodendrocyte apoptosis, activation of microglia/macrophages and axonal damage in the spinal cord (Palumbo and Pellegrini, 2017; Tsunoda and Fujinami, 2010). Demyelination progresses and reaches a plateau at around 100 days post-infection, when infected mice start presenting neurological symptoms such as hind limb weakness, spasticity and gait problems. Afterwards, progressive spinal cord atrophy occurs, which is speculated to result from the loss of medium- and large-diameter axons (McGavern et al., 2000a, 2000b). There is an interesting aspect regarding remyelination in TMEV, which is deemed highly dependent on the mouse strain. Certain mouse strains such as SWR are susceptible to TMEV-IDD but show high capacity for remyelination, with 70% of the lesions showing signs of repair 11 months after TMEV infection. On the other hand, others such as SJL/J (a prototype strain for studying TMEV infection) manifest only 10% remyelination (Bieber et al., 2005; Oleszak et al., 2004). This is similar to what is observed in MS patients, with certain individuals showing spontaneous improvement during the course of the disease, while others progressively decline (Patrikios et al., 2006). The similarities between TMEV-IDD and MS make this model a valuable tool for studying the progressive form of MS, offering an insight into potential myelin reparatory patterns that could have therapeutic value. Furthermore, this model is suitable for investigation of the speculated viral etiology of MS.

Various methods have been used to quantify and measure locomotor behavior in mouse models of neurodegenerative conditions, such as the open field test, tests to assess gait impairments, the balance beam test and rotarod (Dumont, 2011). In MS research, open field locomotion, grid walking, the narrow beam test and measurement of foot exhortation angle have been performed using the EAE model (Buddeberg et al., 2004). In the TMEV model, in addition to qualitative clinical tests that are very subjective (Eldridge et al., 2020; Johnson et al., 2006), the decline in neurological function has been assessed using tools such as spontaneous activity-monitoring box, rotarod, footprint analysis, DigiGait and activity monitoring cage (Bieber et al., 2005; Eldridge et al., 2020; Gilli et al., 2016; McGavern et al., 1999; Mestre et al., 2021; Paz Soldán et al., 2015). Both horizontal and vertical activity have been measured.

Currently, advanced technologies are being developed, with efforts to create automated home cage tests for assessing motor disability and disease progression. Their goal is to reduce variability and user interference during continuous, noninvasive tracking of animals in their home environment (Grieco et al., 2021; Richardson, 2015). Many of these newly developed systems have been applied to study certain phenotypes in animal models of human neurodegenerative diseases (reviewed in (Richardson, 2015). Interestingly, these kinds of studies seem to be less common for MS than for other neurodegenerative diseases. Measuring motor performance in mouse models of MS using automated monitoring systems has been reported for the EAE model (Shahi et al., 2019; Sheridan and Dev, 2014), as well as for TMEV-IDD (Eldridge et al., 2020; Mestre et al., 2021) and the cuprizone model (Cisbani et al., 2021). For TMEV-IDD, as the lengthiest disease model of the three, the majority of data have been obtained only at certain points post-disease induction and for a limited duration of time.

The purpose of this study was to employ one such automated analysis system (Noldus Information Technology, Wageningen, Netherlands) to comprehensively describe TMEV-IDD-induced motor and behavioral phenotypes in two susceptible but differentially remyelinating mouse strains (SJL and SWR) over the entire course of the disease.

2. Materials and methods

2.1. Animals and housing

Twenty-four SJL/J and 24 SWR/J female mice were used for this study. All manipulations were conducted with the approval of the University Animal Ethics Commission (file #20–2229). The SJL mice were supplied by Janvier Laboratories and were shipped at 4 weeks of age. The SWR mice were bred inhouse and weaned at the same age. The mice were kept in an A2 biosecurity-level animal facility under standard housing conditions (humidity 40–60%, temperature 21 °C–24 °C) with a 12 h light/dark cycle (lights on from 7:00 h to 19:00 h). They were provided with standard rodent animal chow and tap water ad libitum. Outside of measurement sessions, the mice were housed in groups of 6 inside a home cage on an IVC rack (Tecniplast). During the recording sessions (once every 2 weeks, each lasting 22 h), each mouse was housed in an individual recording arena (PhenoTyper, Noldus Information Technology, Wageningen, Netherlands). These individual cages were placed in a ventilated cabinet (ARIA BIO C36, Tecniplast) with similar housing conditions as the ones in the IVC rack. For minimizing changes in environmental conditions, the same wooden bricks, black paper stripes (enrichment) and previously autoclaved dark bedding (back-2-nature Small Animal Bedding and Litter, Fibre Cycle AU) were used in home and recording cages, the only difference being that the paper nest was replaced with a plastic shelter in the PhenoTyper arenas. Each mouse was individually identified by an ear punch.

2.2. Induction of TMEV-IDD

At the age of five weeks, 12 SJL/J and 12 SWR/J mice received an intracerebral injection of 12,5 μl of an inoculum containing 2×10^6 pfu/ml of TMEV-DA in DMEM. Twelve SJL/J and 12 SWR/J age-matched mice were injected with the same volume of DMEM only, to serve as mock-infected controls. The injections were performed under deep isoflurane anesthesia in a biosafety cabinet. For induction, mice were placed in a plastic box until adoption of a slow bradypneic respiratory pattern. Next, mice were placed in abdominal position and anesthesia was maintained using a nose adapter supplied with isoflurane ~1%.The intracerebral injection was performed with an insulin syringe (0,3 mL). The site of injection was located midway between the eye and the ear, next to the midline. To avoid excessive penetration and to ensure the correct depth of injection, a modified stop was placed on the needle. Afterwards, the needle was slowly removed to avoid solution leakage. The mice were placed back in their home cage and monitored until they were fully awake. After the injections, the mice were allowed to recover for 5–10 days (they were assessed daily to check for any adverse reactions) until the first group of 12 mice was recorded.

2.3. Phenotyping platform

2.3.1. Description of Noldus video tracking system

For phenotype data acquisition, we used the PhenoTyper cage

coupled with EthoVision XT16 software (Noldus Information Technology, Wageningen, Netherlands), an automated video tracking and motion analysis system that allows uninterrupted tracking of rodents in a home cage environment. Briefly, the detection of the mouse is based on the pixel change between the subject's body and the background. For tracking mice with white fur, the background should be as dark as possible, which is why we used dark bedding material. The experiment was carried out in a custom-made arena called PhenoTyper. This cage consists of a top unit that integrates an infrared lighting system, CCD black/white camera and all the necessary electronic equipment. The infrared lighting array ensures monitoring regardless of ambient light conditions and the video camera continuously captures the movement of the subject. The images are then passed to an associated software platform (EthoVision XT) with different modules for extensive analysis of activity and behavior. For this study we used the PhenoTyper home cage model 3000 (300 × 300 mm) equipped with a top unit, an infrared translucent shelter, a feeder, a drinking bottle, a lickometer and a feeding monitor. This model has 3 plexiglass walls and a front door for easy subject manipulation. The cage bottom comes as a separate part, so we had 2 sets of 12 bottoms to rotate daily. The cage bottoms are black, which ensures that the contrast between the white subject and the background is maintained even if the bedding is being moved around (like when the mouse is digging). The connection between the PhenoTyper and a computer is ensured via an encoder board installed on the workstation. To acquire data in EthoVision XT16 we used tracking licenses (one license required per workstation) that included the Mouse Behavior Recognition Module, Multiple Body Points Module, Multiple Arena Module, and Trial & Hardware Control Module.

2.3.2. Experimental design and analysis settings

The setup consisted of 12 PhenoTypers. Each was connected to a Dell 3630 workstation (4 PhenoTypers per one workstation) on which the software program Ethovision XT16 was installed (Supplementary Information 1.1 and Supplementary information – experimental protocol). This allowed uninterrupted data acquisition in the 12 arenas. Before the start of the experiment, test recordings with noninfected mice were carried out for 1 month to adjust the recording conditions and the detection settings, but also to test how the mice reacted to the recording environment and short-term social isolation. The data acquired were also used to check the software's precision in terms of behavior recognition, by comparing the system's results with manual annotations of the same tracks. The results showed a 70–90% (depending on the behavior) match between manually and automatically scored data, which corresponded to the manufacturer's claims (Supplementary Information 1.2).

Each group of 12 mice underwent a video-tracking session in the PhenoTypers every 14 days over a total of 37 weeks (9 months). The recording sessions lasted 22 h, starting at 15:00 h and finishing at 13:00 h the next day. The two-hour window between recordings was used to return the mice to their home cages, clean the PhenoTypers thoroughly and transfer the next group. The cage bottoms, bedding and water bottles were changed between groups. Each mouse was assigned a PhenoTyper that was labeled with its ear tag ID number to ensure that its follow-up was made in the same arena over the 9 months. For the analysis, we used the mouse behavior recognition module in Ethovision XT16 with center-point, nose-point and tail-base detection. The *contour-based* body detection technique and the dynamic subtraction method for subject detection were applied. The behavioral recognition settings (subject area, center-nose length, center-tail length and posture) were updated before each recording session to take into account body size changes in growing/aging mice. A detailed overview of the used settings is presented in Supplementary information – experimental protocol.

2.3.3. Parameters, data profiles and analysis

The choice of relevant parameters was made by taking into consideration the main hallmarks of TMEV-IDD: progressive motor impairments and waddling gait. The set of parameters related to spontaneous locomotion that were used to monitor the progressive motor impairment are shown in Table 1. As the hind limbs are the most affected in TMEV and are largely responsible for the wobbling gait, we looked at center and tail base-point-related parameters to assess overall gait changes. From the Ethovision XT16 panel we used the *turn angle* of the center and the tail base point (parameters related to "direction"). Further, we derived a new variable by dividing the distance covered by the tail point by the distance covered by the center point and called it the *tail-to-center ratio*. Finally, we assessed parameters describing normal mouse behaviors to check whether (and how) they are altered during the course of TMEV-IDD (Table 1). The said variables were then expressed as mean values over the 22 h-long recording session.

Three analysis profiles with 12 variables were used to assess the acquired data. The frequency and duration of behaviors were analyzed using a data profile with no smoothing or filtering applied ("all data"). Locomotion- and gait-related parameters were analyzed after filtering the data to "walking" or "merged rearing". In this way, data were reduced to only the segments of the track where active horizontal and vertical locomotion occurred, thus eliminating "noise" created by small movements and body turns.

2.4. Statistics

Individual data from each recording week (mean values over 22 h) were entered in GraphPad Prism10.0.2 software and are expressed as the mean ± SEM. Measurements from recording week 5 were taken as a baseline measure[1] for inter- and intra-strain comparisons. A mixed model followed by the Bonferroni post hoc test was used to determine the statistical significance between groups. Values of $p < 0.05$ were considered significant. Simple linear regression was used to determine trends over time (95% confidence interval).

3. Results

3.1. Spontaneous locomotion

3.1.1. Horizontal locomotion

The three horizontal locomotion values (HLVs) displayed similar trends after infection, with a far more severe decline in SJLs (Fig. 1). ^{v}SJLs HLVs, including distance covered (DC), walking velocity (WV) and walking frequency (WF), significantly declined with time post-infection (Fig. 1A and B). Their collapse (as compared to a baseline set at week 5 pi) was particularly pronounced during the last two months of the observation period (week 27-week 37 pi) (Fig. 1C; Suppl. Tables 1.1, 1.2 and 1.3). Unexpectedly, some HLVs declined with time in age-matched ^{m}SJLs as well (Fig. 1B), with significant decreases in DC and WF, whereas WV remained stable. These observations suggest that repeated observation sessions gradually extinguished the impulse to explore the arena in healthy SJL mice, but without affecting their WV. Furthermore, if the lack of interest in the arena was likely to be the same in diseased SJLs (although the decline was more marked), there was also a drastic reduction in WV, particularly from week 29 pi onwards (Fig. 1C, Suppl. Table 1.2). By the last recording week pi (week 37), ^{m}SJLs had maintained 98.91% of their baseline velocity as opposed to ^{v}SJL's 80.98% ($p < 0.0001$). In ^{v}SWRs, HLVs evolved in a different manner (Fig. 1A and B). They were maintained until the last recording week, when DC and WF, but not WV, significantly declined from baseline (Fig. 1C; Suppl. Tables 1.1, 1.2 and 1.3). In sharp contrast to ^{m}SJLs, age-matched ^{m}SWRs displayed an increase in HLVs, showing no apparent loss of exploratory behavior. A marked difference in HLVs was present between the two

[1] Baseline measurement choice explanation: 1) At week 1 and week 3 mice were still in the acute phase of TMEV, which might have influenced certain parameters. 2) By week 5, mice had already gone to the PhenoTypers at least two times, so they had a chance to accommodate to the recording environment

Table 1
Variables and data profiles used for data analysis in EthoVision XT16.

Variable	Filter/Data profile	Unit	Description	Function
Total distance covered by the center and tail point	Walking	cm	The distance traveled by the center and the tail point of the subject from the previous sample to the current one.	Measure of spontaneous activity -horizontal
Velocity (mean)	Walking	cm/s	The distance moved by the center, nose or tail-base point of the subject per unit time.	Measure of spontaneous activity - horizontal
Walking	All data	Frequency Duration (in seconds)	The subject moves to another place, and hind legs move as well.	Measure of spontaneous activity - horizontal
Rearing unsupported	All data	Frequency Duration (in seconds)	The subject stands in an upright posture, with front paws not in contact with any object. Includes the rise and descent.	Measure of spontaneous activity - vertical
Velocity (mean)	Supported and unsupported rearing in arena and wall zone	cm/s	The distance moved by the center, nose or tail-base point of the subject per unit time.	Measure of spontaneous activity - vertical
Tail-center ratio	Walking	Ratio	Ratio between the distance covered by the tail and the distance covered by the center point.	Gait assessment
Turn angle of center and tail point	Walking	Deg	The change in direction of the nose, center and tail-base point between two consecutive samples.	Gait assessment
Eating	All data	Frequency Duration (in seconds)	The subject eats at the feeder or from the floor or is eating while holding food in front paws.	Maintenance behavior
Grooming	All data	Frequency Duration (in seconds)	The subject grooms snout, head, fur or genitals. Includes scratching and licking of paws during a grooming session.	Maintenance behavior
Rearing supported	All data	Frequency Duration (in seconds)	The subject stands in an upright posture, leaning with front paws against the cage wall. Includes the rise and descent.	Exploratory behavior
Sniffing	All data	Frequency Duration (in seconds)	The subject makes slight movements of the head, possibly with slight, discontinuous body displacement. Includes sniffing the air, the wall, the floor and other objects.	Exploratory behavior
Resting	All data	Frequency Duration (in seconds)	The subject rests with hardly any movement, either sits or lays down. Includes sleeping. Apparently, no interest in the environment.	Inactive behavior

TMEV-infected strains during the last two months of the observation period. By week 37 pi, ^{v}SWRs still accomplished ~64%, ~93% and 70% of baseline DC, WV and WF, while ^{v}SJLs reached only ~45%, ~81% and ~ 54%, respectively (Fig. 1C; Suppl. Tables 1.1, 1.2 and 1.3).

3.1.2. Vertical locomotion

Vertical locomotion values (VLVs) largely mirrored HLVs. We assessed the unsupported rearing frequency (URF) when mice used only their hind legs as a support, as well as the total rearing velocity of the center point (TRV), including both supported and unsupported rearing instances in the arena and wall zone.

^{v}SJLs showed a first significant decline in TRV at week 13 pi (87.51% from baseline, $p < 0.0001$). The first decrease in URF was noted at week 15 pi, but this was not significant (69% from baseline, $p = 0.2467$). In the late chronic stage, starting from week 23 pi, both VLVs significantly reduced compared to baseline (Fig. 2C; Suppl. Tables 2.1 and 2.2). ^{m}SJLs also decreased their URF in the final stages but their TRV remained stable. By the last point of observation (week 37 pi), both groups had significantly reduced their URF, with ^{m}SJLs having 57.3% ($p = 0.0063$) and ^{v}SJLs only 39.95% ($p < 0.0001$) of their baseline performances (Suppl. Table 2.1). ^{m}SJLs, however, maintained 96.37% ($p > 0.9999$) of their baseline TRV, as opposed to ^{v}SJL's 87.48% ($p < 0.0001$) (Suppl. Table 2.2).

Consistent with their HLVs, ^{m}SWR mice also increased their VLVs with time, while ^{v}SWRs maintained them up until the last recording week (Fig. 2A and B; Suppl. Tables 2.1 and 2.2).

As opposed to ^{v}SJLs, for whom progressive decline was observed during the entire late chronic phase, vertical activity, especially TRV, remained relatively stable in ^{v}SWRs up until the last week of recording, when VLVs dropped significantly (Fig. 2C; Suppl. Tables 2.1 and 2.2). At the last observation point (week 37 pi), ^{v}SJLs reached 39.95% ($p < 0.0001$) and 87.48% ($p = 0.0002$) of baseline URF and TRV, respectively, while ^{v}SWRs reached 58.71% ($p = 0.0038$) and 88.89% ($p = 0.0008$).

These data suggest that, despite being affected by the virus towards the end stages, ^{v}SWRs were able to maintain their spontaneous horizontal and vertical activity levels longer than ^{v}SJLs. Furthermore, the % reduction in performance from baseline was milder compared to ^{v}SJLs and their overall spontaneous activity was relatively preserved. Moreover, control mice data demonstrate that other variables, besides TMEV infection, such as aging and recording environment, can affect certain aspects of spontaneous locomotion in both strains.

3.2. Gait

The most obvious clinical symptom following TMEV infection in mice is a wobbling gait. We attempted to assess and quantify the gait alterations (GAs) in Ethovision 16, using measurements such as the turn angle of the center point (TACP), turn angle of the tail base point (TATP) and ratio of the distance covered by the tail base point and the center point (TCR).

In ^{v}SJL mice, all gait assessment values (GAVs) increased with time (Fig. 3A and B). The first significant increases compared to baseline were seen at week 11 and week 13 pi ($p < 0.0001$, Fig. 3C), which matches the time of peak TMEV-induced demyelination described elsewhere. A second period of increase was evident in the late chronic stage (Fig. 3C). The highest increase was observed at recording week 33 with 23.4%, 27.3% and 32.8% of baseline TACP, TATP and TCR, respectively ($p < 0.0001$, Fig. 3C, Suppl. Tables 3.1,3.2,3.3). Age-matched ^{m}SJLs did not demonstrate significant increases from baseline in GAVs at any time point (Fig. 3A; Suppl. Tables 3.1, 3.2 and 3.3). Very significant differences between ^{v}SJLs and ^{m}SJLs ($p < 0.0001$) were observed at recording weeks 11, 13, 15, 19, 31, 33, 35 and 37 pi (Suppl. Tables 3.1, 3.2 and 3.3).

Similar to ^{v}SJLs, in ^{v}SWRs, GAVs also increased with time pi (Fig. 3A and B). The first very significant increase from baseline (in TATP) was at week 7 pi ($p < 0.0001$; Fig. 3C). From week 21 pi onwards, GAVs significantly increased compared to baseline values. Peak values were

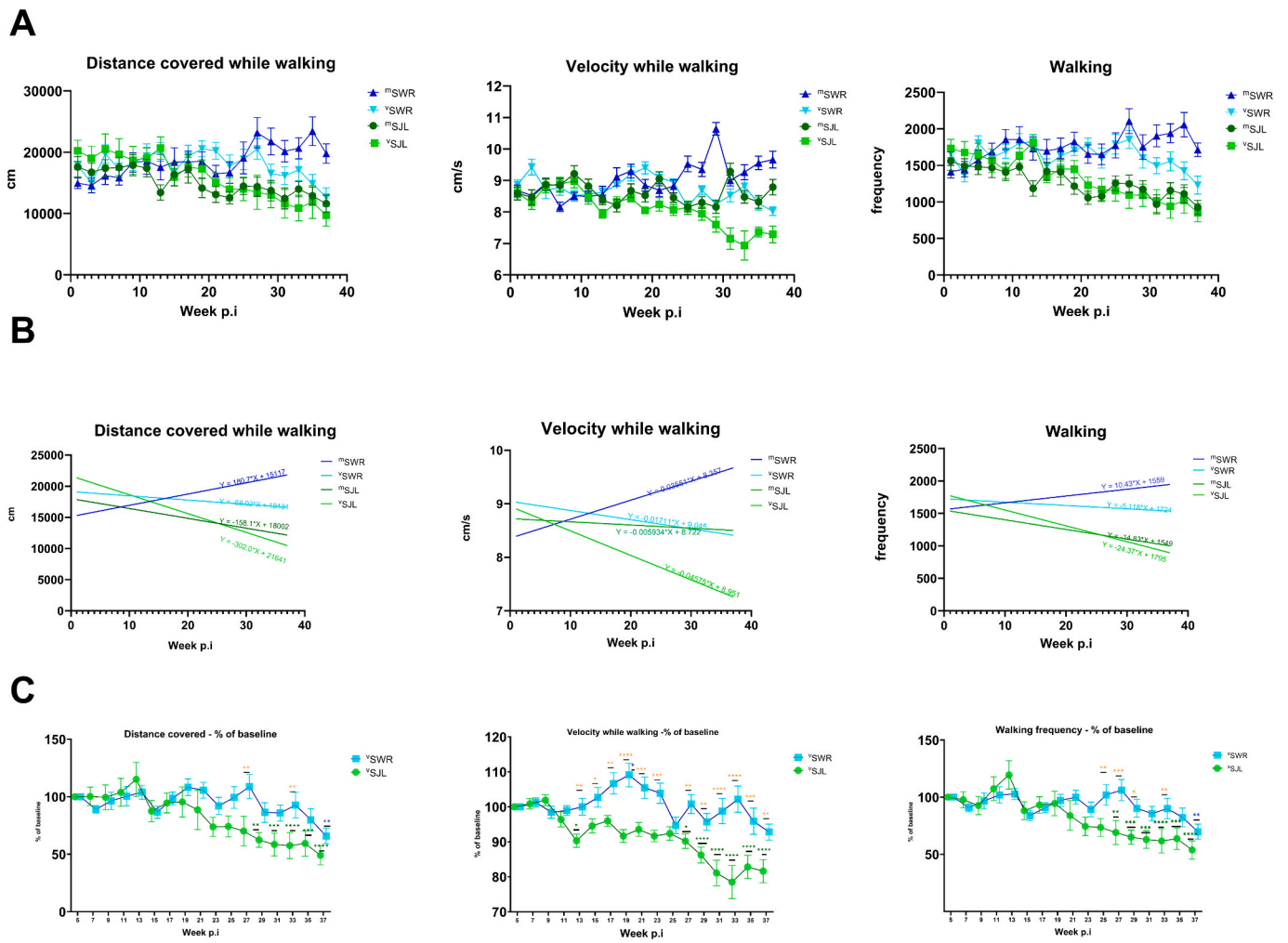

Fig. 1. Progression of horizontal spontaneous activity for 37 weeks post-TMEV-infection.
A: Measurement of horizontal activity over 22 h every 2 weeks. Mean + SEM of 12 mice per group for each data point post-infection. B: Simple linear regression displaying how time post-infection affects parameters quantifying horizontal activity. ^{v}SJLs (DC $r^2 = 0.91$, $p < 0.0001$; WV $r^2 = 0.76$, $p < 0.000$; WF $r^2 = 0.87$, $p < 0.0001$), ^{m}SJLs (DC $r^2 = 0.70$, $p < 0.0001$; WV $r^2 = 0.04$, $p = 0.4219$; WF $r^2 = 0.75$, $p < 0.0001$), ^{v}SWRs (DC $r^2 = 0.12$, $p = 0.1397$; WV $r^2 = 0.24$, $p = 0.0328$; WF $r^2 = 0.1$, $p = 0.1564$), ^{m}SWRs (DC $r^2 = 0.65$, $p \leq 0.0001$; WV $r^2 = 0.49$, $p = 0.0009$; WF $r^2 = 0.43$, $p = 0.0021$). C: Interstrain comparison between TMEV-infected mice; data presented as % of baseline values. Stars indicate, for the corresponding time point, a statistically significant difference ($p < 0.05$) between infected strains (orange), statistically significant difference from baseline for ^{v}SJL (green) and statistically significant difference from baseline for ^{v}SWR (blue). ^{v}SJLs – virus-infected SJLs, ^{m}SJLs – mock-infected SJLs, ^{v}SWRs – virus-infected SWRs, ^{m}SWRs – mock-infected SWRs, DC - distance covered, WV - walking velocity, WF - walking frequency. (For interpretation of the references to colour in this figure legend, the reader is referred to the web version of this article.)

reached at week 37 pi, when ^{v}SWR mice had increases of 25.6%, 20.2% and 19.4% of baseline TACP, TATP and TCR, respectively ($p < 0.0001$; Fig. 3C; Suppl. Tables 3.1, 3.2 and 3.3). On the contrary, age-matched ^{m}SWR mice did not demonstrate significant increases from baseline at any time point (Fig. 3A and B and Suppl. Tables 3.1, 3.2 and 3.3). Very significant differences between ^{m}SWRs and ^{v}SWRs ($p < 0.0001$) were observed at recording weeks 7, 21, 23, 27, 29, 31, 33, 35 and 37 (Suppl. Tables 3.1, 3.2 and 3.3).

The pattern of gait alterations differed in the two infected strains. While ^{v}SJL mice had a biphasic increase in GAVs with early- and late-stage augmentations, ^{v}SWR mice displayed a progressive increase in GAV as the disease advanced to the late chronic phase (Fig. 3C and Suppl. Tables 3.1, 3.2, and 3.3.3).

3.3. Behavior

We grouped common measurable behaviors into two categories, according to a mouse ethogram described elsewhere (https://mousebehavior.org/active-behavior/): maintenance (eating and grooming) and exploration (rearing, sniffing and resting).

3.3.1. Eating and grooming

Maintenance behaviors are active behaviors that typically function to maintain the physiological state, comfort and appearance of the mouse (cited from https://mousebehavior.org/maintenance-behavior). To assess this, we measured the frequency of eating and grooming.

In ^{v}SJLs, eating frequency (EF) remained stable throughout the course of the disease (Fig. 4A and B; Suppl. Table 4.1), with no significant reductions from baseline. Curiously, ^{m}SJLs had decreased EF with time (Fig. 4A and B; Suppl. Table 4.1), but without significant differences from baseline. This was also confirmed by the fact that none of the groups had lost weight since the start of the experiment. ^{v}SWR mice had a slight decrease in EF (Fig. 4A and B), but without significant reductions from baseline (Fig. 4C; Suppl. Table 4.1). This was different from their mock-infected controls, who significantly increased their food consumption (Fig. 4A and B; Suppl. Table 4.1).

The frequency of grooming (GF) increased in both ^{v}SJLs and ^{m}SJLs (Fig. 4A and B). Interestingly, in ^{v}SJLs, there was a noticeable (14% from

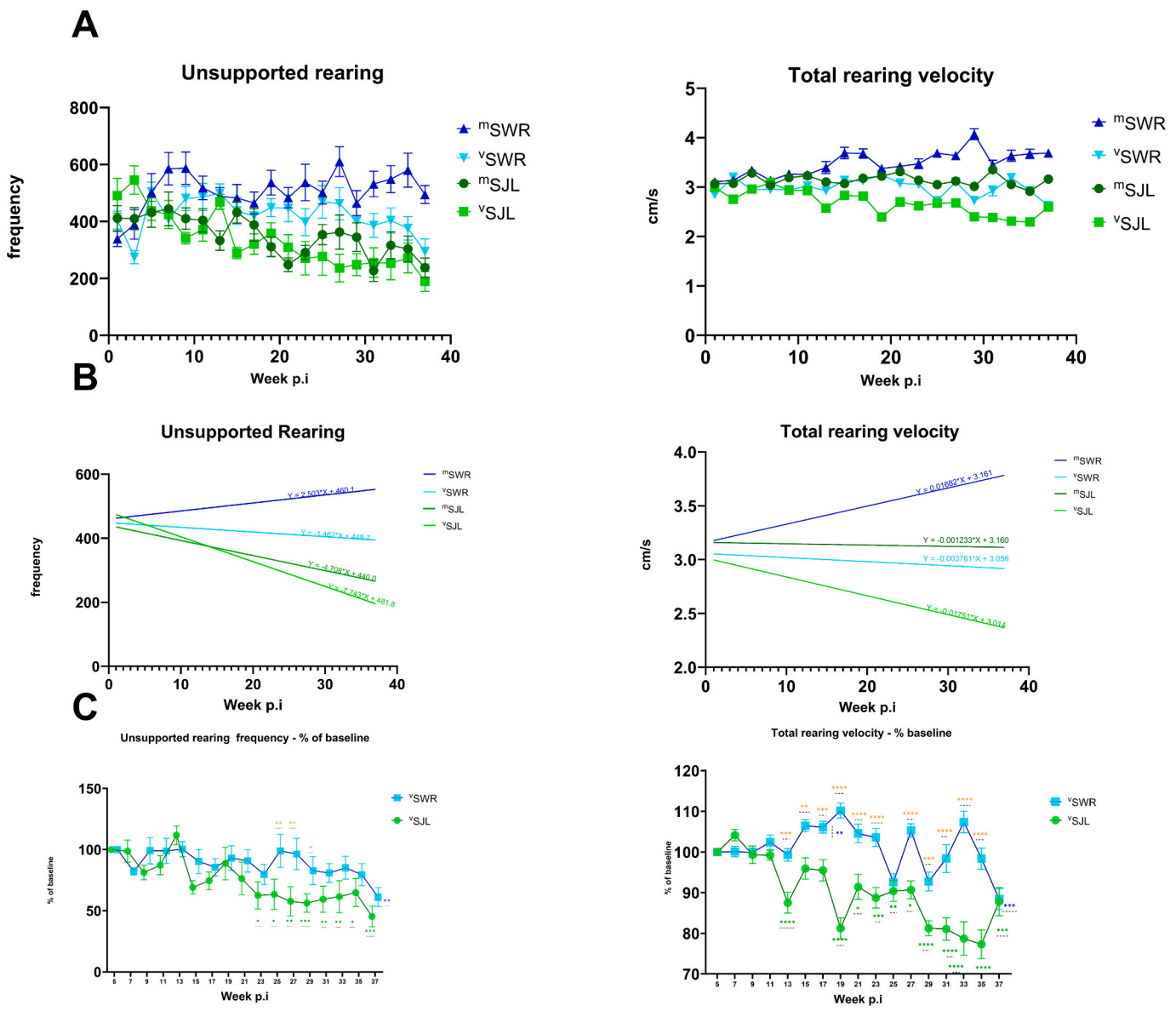

Fig. 2. Progression of vertical spontaneous activity for 37 weeks post-TMEV-infection.
A: Measurement of vertical activity for 22 h every second week. Mean + SEM of 12 mice per group for each data point post-infection. B: Simple linear regression displaying how time post-infection affects parameters quantifying vertical activity. ^{v}SJLs (URF $r^2 = 0.79$, $p < 0.0001$; TRV $r^2 = 0.65$, $p < 0.0001$), ^{m}SJLs (URF $r^2 = 0.59$, $p < 0.0001$; TRV $r^2 = 0.01$, $p = 0.6110$), ^{v}SWRs (URF $r^2 = 0.07$, $p = 0.2714$; TRV $r^2 = 0.06$, $p = 0.3055$), ^{m}SWRs (URF $r^2 = 0.17$, $p = 0.0718$; TRV $r^2 = 0.58$, $p = 0.0002$). C: Interstrain comparison between TMEV-infected mice, data presented as % of baseline values. Stars indicate, for the corresponding time point, a statistically significant difference ($p < 0.05$) between infected strains (orange), statistically significant difference from baseline for ^{v}SJL (green) and statistically significant difference from baseline for ^{v}SWR (blue). ^{v}SJLs – virus-infected SJLs, ^{m}SJLs – mock-infected SJLs, ^{v}SWRs – virus-infected SWRs, ^{m}SWRs – mock-infected SWRs, URF - unsupported rearing frequency, TRV - total rearing velocity. (For interpretation of the references to colour in this figure legend, the reader is referred to the web version of this article.)

baseline) but statistically insignificant increase in GF at week 13, coinciding with the peak in wobble and first drop in velocity of walking and rearing. A significant increase from baseline (26%, $p = 0.0024$) was noted at the last recording week (Fig. 4C, Suppl. Table 4.2). On the other hand, GF remained stable in both ^{v}SWR and ^{m}SWR mice (Fig. 4A and B; Suppl. Table 4.2), indicating that strain-specific factors might influence this parameter.

Taken together, the data suggest that TMEV infection does not affect maintenance behaviors and that infected mice are able to express normal behavior throughout most of the disease course.

3.3.2. *Rearing, sniffing and resting*

Two parameters were used to measure active exploratory behavior: supported rearing frequency (SRF) and sniffing frequency (SF). We also looked at the resting duration (RD) as a measure of inactive behavior.

^{v}SJL mice demonstrated a significant decline in their active exploratory behavior for both SRF and SF, as well as an increase in RD (Fig. 5A and B). While a similar decrease for active exploration was seen in the age-matched ^{m}SJL mice, RD remained stable (Fig. 5A and B; Suppl. Tables 5.1, 5.2 and 5.3).

In ^{v}SWR mice, active exploration decreased, as opposed to their age-matched controls (Fig. 5A and B; Suppl. Tables 5.1 and 5.3). Resting duration did not change in ^{v}SWR but it decreased in ^{m}SWR (Fig. 5A and B), consistent with their overall robust activity.

Overall, the two infected strains displayed similar changes in exploratory activity. Both ^{v}SJL and ^{v}SWR mice reduced their exploration

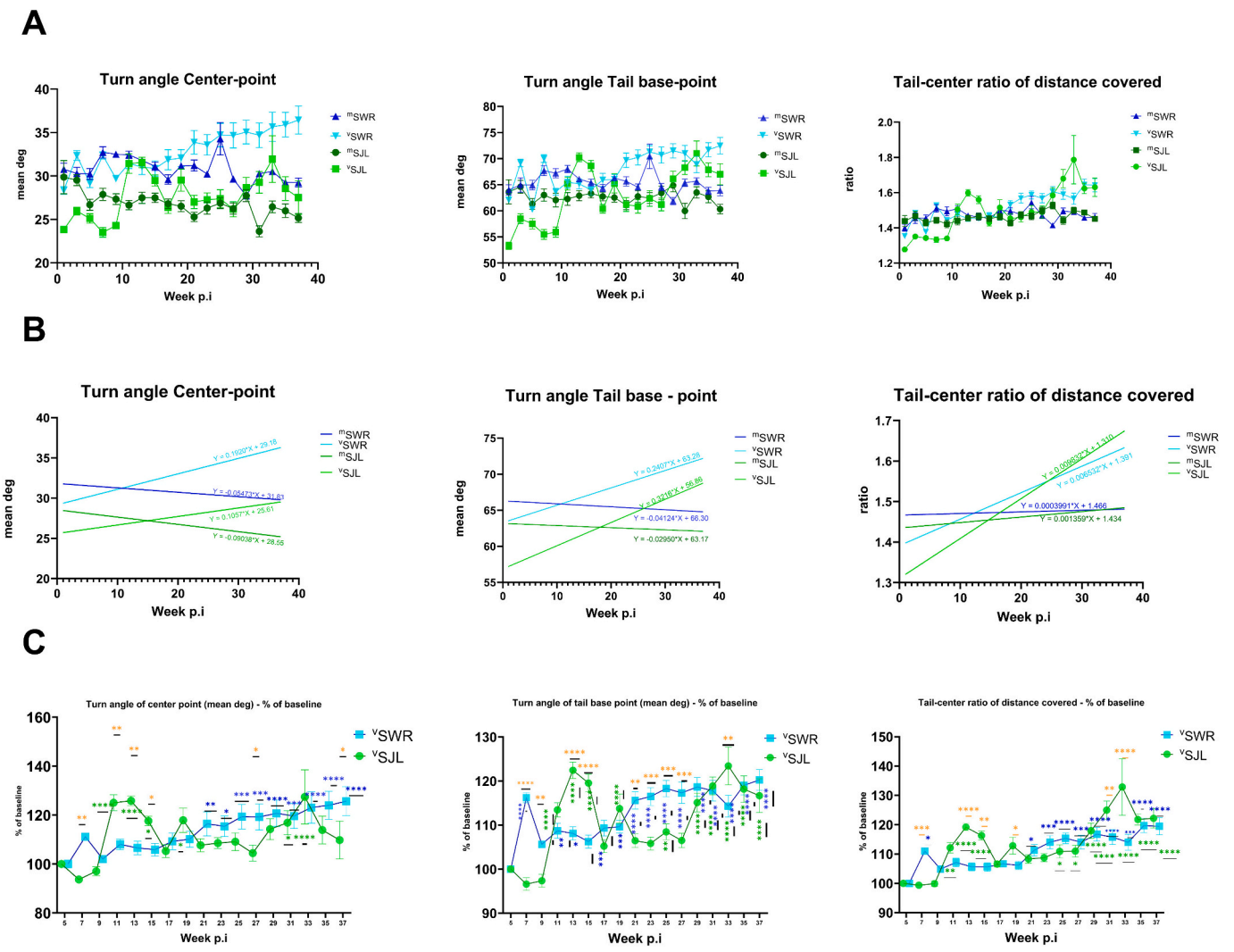

Fig. 3. Monitoring of gait alterations for 37 weeks post-TMEV-infection.
A: Measurement of gait-related parameters for 22 h every second week. Mean + SEM of 12 mice per group for each data point post-infection. B: Simple linear regression displaying how time post-infection affects parameters quantifying gait. ^{v}SJLs (TACP $r^2 = 0.21$, $p = 0.0429$; TATP $r^2 = 0.46$, $p = 0.0013$; TCR $r^2 = 0.68$, $p < 0.0001$), ^{m}SJLs (TACP $r^2 = 0.51$, $p = 0.0006$; TATP $r^2 = 0.06$, $p = 0.2783$;TCR $r^2 = 0.30$, $p = 0.0137$), ^{v}SWRs (TACP $r^2 = 0.83$, $p < 0.0001$; TATP $r^2 = 0.55$, $p = 0.0003$; TCR $r^2 = 0.77$, $p < 0.0001$), ^{m}SWRs (TACP $r^2 = 0.16$, $p = 0.0831$; TATP $r^2 = 0.06$, $p = 0.3097$; TCR $r^2 = 0.01$, $p = 0.5854$). C: Interstrain comparison between TMEV-infected mice; data presented as % of baseline values. Stars indicate, for the corresponding time point, a statistically significant difference ($p < 0.05$) between infected strains (orange), statistically significant difference from baseline for ^{v}SJL (green) and statistically significant difference from baseline for ^{v}SWR (blue). ^{v}SJLs – virus-infected SJLs, ^{m}SJLs – mock-infected SJLs, ^{v}SWRs – virus-infected SWRs, ^{m}SWRs – mock-infected SWRs, TACP - turn angle of the center point, TATP - turn angle of the tail base point, TCR – ratio of distance covered by tail base point and center point. * Increase in TACP and TATP (A) in ^{m} SWRs at week 25 was due to power supply failure that led to suboptimal detection *. (For interpretation of the references to colour in this figure legend, the reader is referred to the web version of this article.)

compared to baseline levels in the later stages of TMEV-IDD, starting from week 29 pi onwards. At the last recording week, both SRF and SF in infected mice diminished significantly ($p < 0.0001$) compared to baseline (Fig. 5C; Suppl. Tables 5.1 and 5.3). ^{v}SJL mice, however, seemed to spend more time inactive (resting) as the disease progressed, compared to both ^{m}SJL and ^{v}SWR mice (Fig. 5C, Suppl. Table 5.2).

4. Relationship between spontaneous locomotion and gait parameters – summary of results

A strong negative correlation was apparent between the velocity while walking and the three gait parameters in ^{v}SJL mice, especially for the tail center ratio ($r = -0.79$). In comparison, this correlation was weak in their mock-infected counterparts (Fig. 6). ^{v}SWR mice displayed a mild negative correlation between distance covered while walking and gait alterations.

This underlines how the progression of TMEV-IDD in the ^{v}SJL mice is characterized by a simultaneous decrease in spontaneous locomotion and an increase in gait disturbances. On the other hand, although ^{v}SWR mice showed progressive gait disturbances, their velocity while walking remained relatively stable even if the total distance that they covered decreased.

5. Heatmaps and path visualization

In addition to the quantification of locomotion and behavior, Ethovision offers a unique opportunity to visualize the acquired data. The video files can be used for validation and verification purposes, troubleshooting or adjusting recording conditions. The heatmaps and track images support the numerical data output with a real-time illustration of the subject's path or level of activity.

In Fig. 7, the heatmaps show how horizontal activity (walking) in

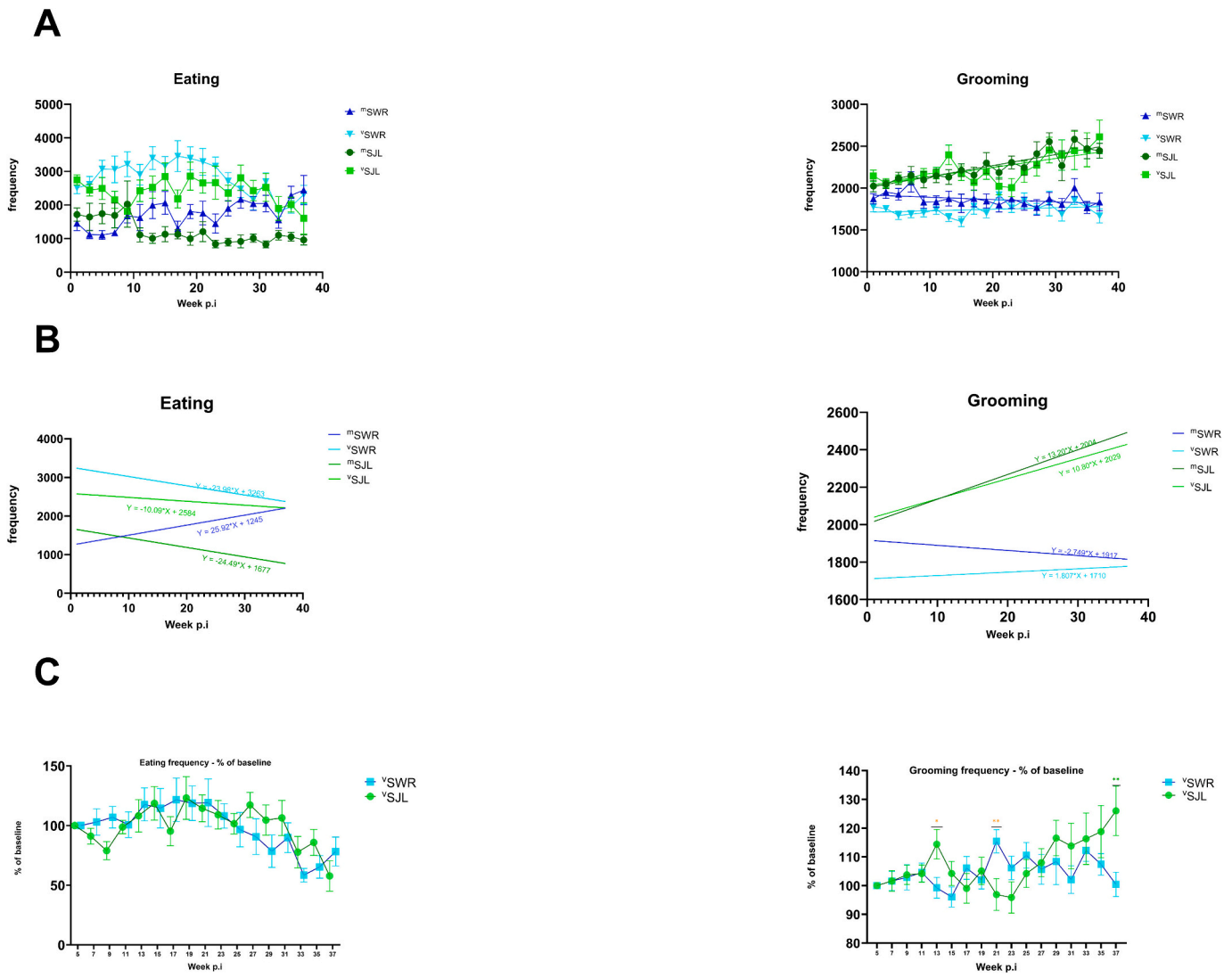

Fig. 4. Monitoring of maintenance behavior for 37 weeks post-TMEV-infection.
A: Measurement of eating and grooming for 22 h every second week. Mean + SEM of 12 mice per group for each data point post-infection. B: Simple linear regression displaying how time post-infection affects parameters quantifying maintenance behavior. ^{v}SJLs (EF $r^2 = 0.09$, $p = 0.1922$; GF $r^2 = 0.48$, $p = 0.001$), ^{m}SJLs (EF $r^2 = 0.58$, $p = 0.0001$; GF $r^2 = 0.78$, $p < 0.0001$), ^{v}SWRs (EF $r^2 = 0.29$, $p = 0.0175$; GF $r^2 = 0.06$, $p = 0.2902$), ^{m}SWRs (EF $r^2 = 0.5324$, $p = 0.0004$; GF $r^2 = 0.1571$, $p = 0.0929$). C: Interstrain comparison between TMEV-infected mice; data presented as % of baseline values. Stars indicate, for the corresponding time point, a statistically significant difference ($p < 0.05$) between infected strains (orange), statistically significant difference from baseline for ^{v}SJL (green) and statistically significant difference from baseline for ^{v}SWR (blue). ^{v}SJLs – virus-infected SJLs, ^{m}SJLs – mock-infected SJLs, ^{v}SWRs – virus-infected SWRs, ^{m}SWRs – mock-infected SWRs, EF - eating frequency, GF - grooming frequency. (For interpretation of the references to colour in this figure legend, the reader is referred to the web version of this article.)

^{v}SJL mice diminished as TMEV progressed, while gait alterations became more evident. The same can be seen in the supplementary video material.

6. Discussion

In this study, we have presented a novel way of quantifying locomotor deficits, gait alterations and behavioral changes in the well-established TMEV mouse model of multiple sclerosis. For that purpose, we employed a video tracking tool (Noldus IT) that followed the nine-month progression of TMEV-induced demyelinating disease in two inbred mouse strains.

For many years, the assessment of motor impairments in the TMEV model has been performed using qualitative tests (Eldridge et al., 2020; Johnson et al., 2006). Although they are useful, these tests are highly subjective and thus not reliable enough to use as a sole tool. Alternatively, the quantification of locomotor deficits to track TMEV progression has been attempted using different methods and protocols (Bieber et al., 2005; Gilli et al., 2016; McGavern et al., 1999; McGavern et al., 2000a, 2000b; Paz Soldán et al., 2015).

The rotarod apparatus is one of the most commonly used tools for motor assessment in the TMEV model. This behavioral test is used to assess various motor-associated functions and locomotor performance in rodents (Crawley, 2003). Despite its superiority over conventional visual qualitative tests, this method has many limitations, including low inter-laboratory reliability, training requirements, extensive setup, limited duration trials and mouse weight considerations (Gilli et al., 2016; Brooks and Dunnett, 2009). Moreover, from our own experience and that of others (Chauffray, unpublished observations; Brooks and Dunnett, 2009), rotarod performance is highly motivation-driven depending on the mouse strain: both mock and infected SWR mice refused to perform the test by falling off or jumping the rod immediately

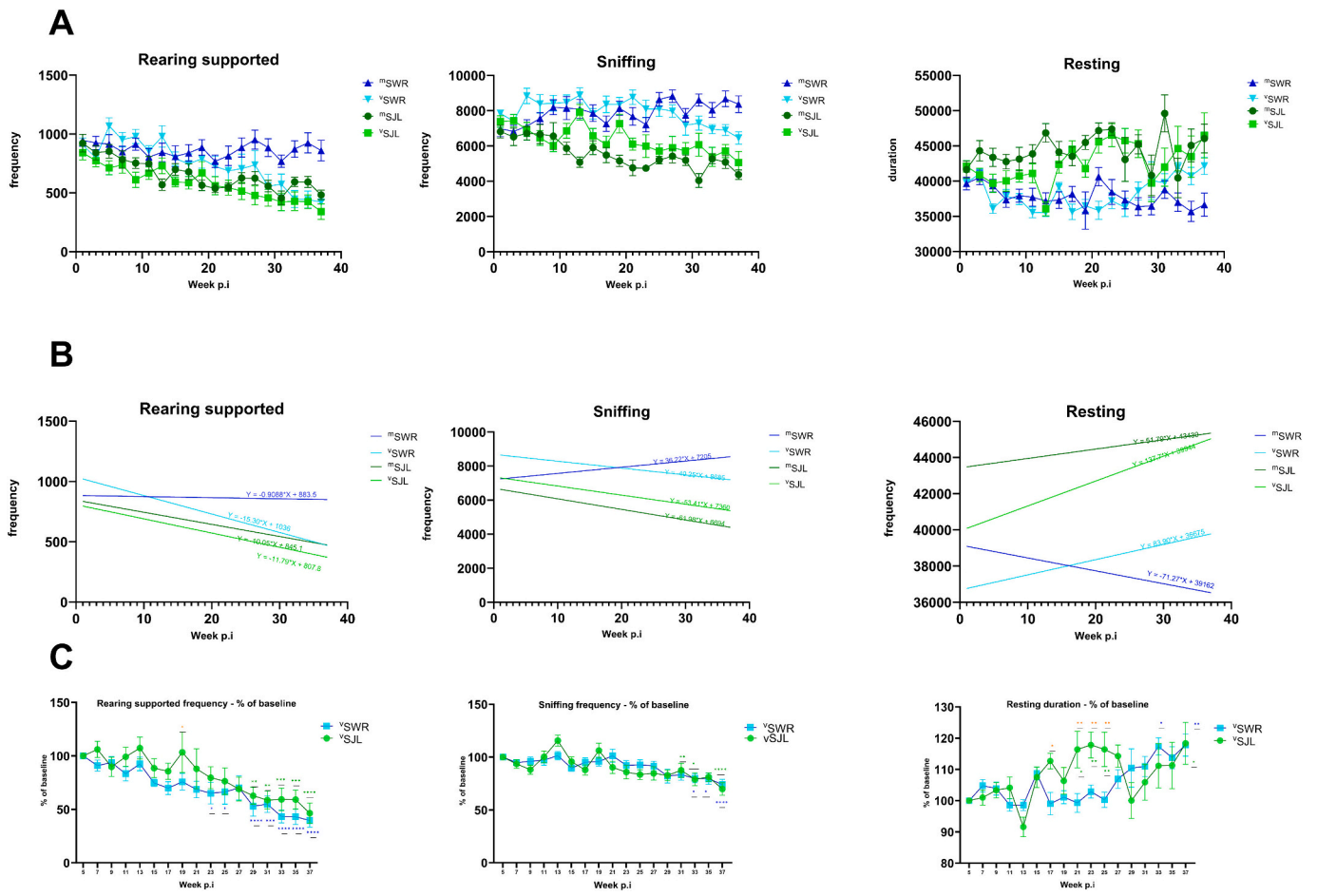

Fig. 5. Measurement of exploratory behavior and resting for 37 weeks post-TMEV-infection.
A: Measurement of rearing supported, sniffing and resting for 22 h every second week. Mean + SEM of 12 mice per group for each data point post-infection. B: Simple linear regression displaying how time post-infection affects parameters quantifying exploration. ^{v}SJLs (SRF $r^2 = 0.91$, $p < 0.000$; SF $r^2 = 0.61$, $p < 0.0001$; RD $r^2 = 0.30$, $p = 0.0140$), ^{m}SJLs (SRF $r^2 = 0.74$, $p < 0.0001$; SF $r^2 = 0.71$, $p < 0.0001$; RD $r^2 = 0.06$, $p = 0.3049$), ^{v}SWRs (SRF $r^2 = 0.81$, $p < 0.0001$; SF $r^2 = 0.40$, $p = 0.0032$; RD $r^2 = 0.17$, $p = 0.0761$), ^{m}SWRs (SRF $r^2 = 0.03$, $p = 0.4543$; SF $r^2 = 0.45$, $p = 0.0017$; RD $r^2 = 0.30$, $p = 0.0142$). C: Interstrain comparison between TMEV-infected mice; data presented as % of baseline values. Stars indicate, for the corresponding time point, a statistically significant difference ($p < 0.05$) between infected strains (orange), statistically significant difference from baseline for ^{v}SJL (green) and statistically significant difference from baseline for ^{v}SWR (blue). ^{v}SJLs – virus-infected SJLs, ^{m}SJLs – mock-infected SJLs, ^{v}SWRs – virus-infected SWRs, ^{m}SWRs – mock-infected SWRs, SRF- supported rearing frequency, SF- sniffing frequency, RD-resting duration. (For interpretation of the references to colour in this figure legend, the reader is referred to the web version of this article.)

upon starting, rendering the obtained results unreliable. In addition, mice from this strain showed visible stress when handled for a prolonged time. This was one of the main reasons why we opted for a video-tracking-based method to track TMEV progression, especially one that is not dependent on the subject's motivation to perform and measures spontaneously occurring behaviors. While rotarod measures latency to fall as the main output of motor evaluation, Ethovision offers a panel of parameters that quantify horizontal and vertical displacement based on the tracking of the subject's center point. Furthermore, data collection can be achieved without a constant human presence, which decreases workload while also reducing human interference.

Recently, the advancement of technology has led to the development of automated systems that measure spontaneous locomotion and behavior. The advantages of employing such systems are numerous: prolonged, unbiased observations of spontaneous behavior; continuous monitoring during all phases of the circadian cycle; studying subjects in a familiar environment; less novelty-related interferences; minimization of handling-provoked stress; simultaneous measurements of more parameters; evaluation of the translational value of preclinical disease models and many more. Limitations in using automated systems also exist, such as the need for solitary housing of subjects to obtain individual measurements, lack of a uniform recording system that contributes to result disparities between laboratories, limitation/omission of environmental enrichment during acquisition, large data output that might be difficult to analyze and store, and costs associated with the purchase and setup of equipment (Grieco et al., 2021; Haynell and Marklund, 2014; Richardson, 2015; Voikar and Gaburro, 2020).

Different home cage monitoring systems can be found on the market and the PhenoTyper from Noldus was best suited to our requirements (longitudinal study, uninterrupted measurement of spontaneous locomotory behavior at regular intervals, reproducible data results, video image of the actual state, individual measurements), with the main limitation being the social isolation of mice during data acquisition. We opted for 22-h-long recording sessions in order to capture almost one whole circadian cycle and to allow for gradual habituation to the recording environment.

As stated above, the main advantage of using the Noluds video tracking platform over the traditional Rotarod test is the non-invasive measurement of spontaneous occurring behaviors in mice. In comparison with other home cage monitoring systems (such as TSE – IntelliCage) that use radiofrequency identification (RFID) technology, in EthoVision XT 16 the subject is followed by contour-based video analysis which is non-invasive. Furthermore, compared to technologies who use infrared sensors (The SmartCage™, The PhenoMaster), the Noldus platform gives

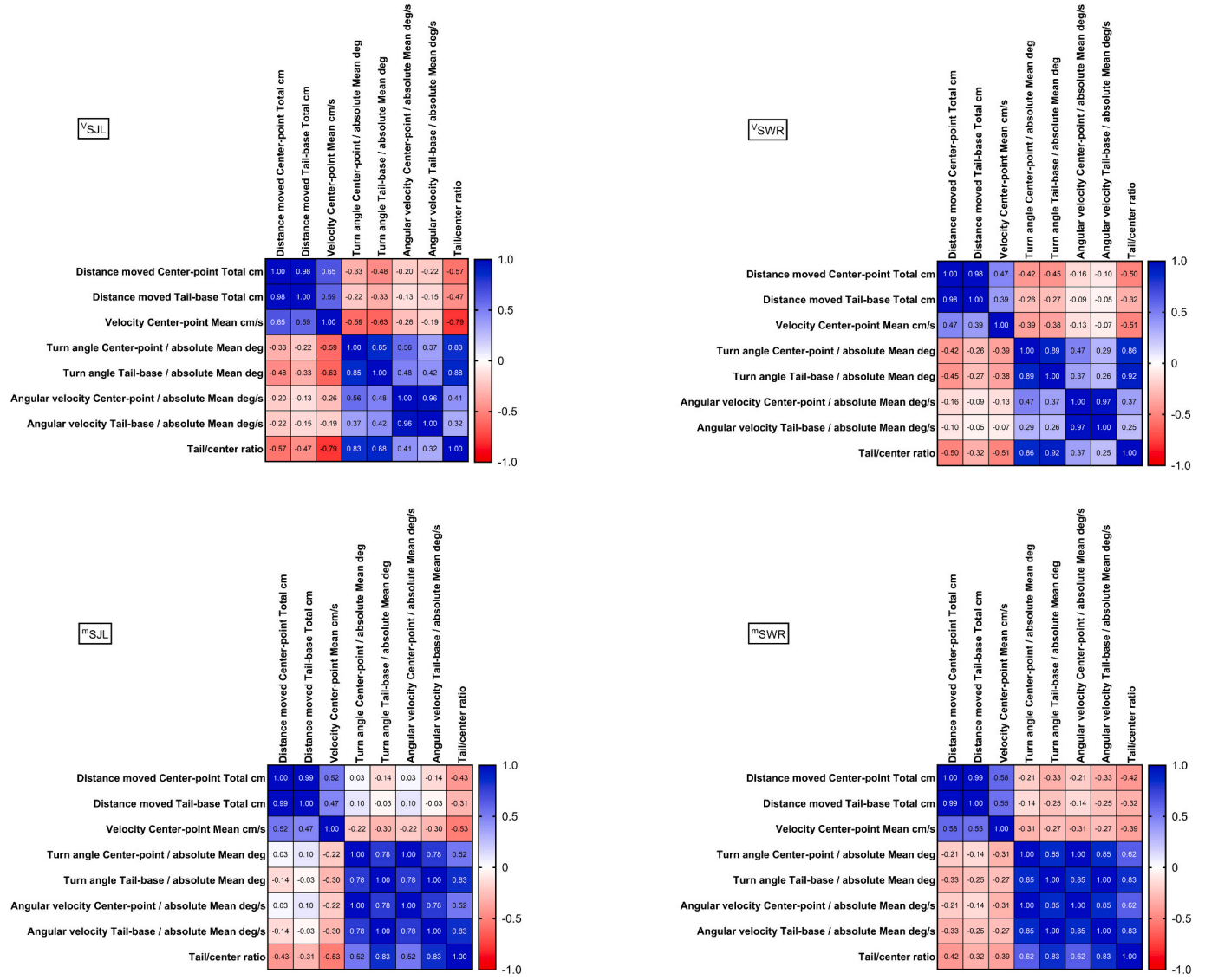

Fig. 6. Correlation matrix showing relationships between parameters quantifying horizontal spontaneous locomotion and gait alterations for both infected strains and their controls.
Pearson r correlation coefficients shown.

a visual output of the data in addition to the numerical output, thus confirming the authenticity of the latter. A detailed comparison of commonly used automated systems, including this one, is comprehensively described by (Robinson and Riedel, 2014).

The main disadvantage of this automated system is housing each mouse individually during the recording sessions. Mice are social animals and social isolation could impact specific behaviors. A recent study (Bass et al., 2020) has demonstrated that individual housing of C57BL/6 J mice in PhenoTypers for 8 days resulted in decrease of overall activity. However, it appears that this decline (for total daily distance) was only apparent starting on day 4. Our protocol included <24 h of social isolation before mice were returned to their established home cage social groups.

A limitation of this platform can be the initial price to obtain it. Low-cost video tracking systems using cameras and free software exist and are certainly more affordable compared to commercial options. However, the validation process and troubleshooting are laborious and there is always a question of reproducibility of the results depending on the setup. Furthermore, commercial systems such as the Noldus platform are better suited for longitudinal studies.

The second limitation is the high throughput of data acquired through 22 h of recordings. Large amounts of data can be difficult to store and take time to process. This can be addressed in EthoVision XT by the option to filter and export only data segments and behaviors of interest depending on further analysis.

The use of automated home cage systems has also been reported in respect of the other two mouse models of MS. The elegant study of (Cisbani et al., 2021) describes the use of the automated system Intellicage in the cuprizone model. They demonstrated that cuprizone-fed B6 mice decrease their spontaneous activity, especially the velocity of movement, compared to controls. This is in line with our results on reduced velocity in TMEV-infected as opposed to mock-infected SJL mice.

Another study (Shahi et al., 2019) used the IRAMS system in the EAE model of MS to assess nocturnal rearing as a marker for scoring disease activity. It was found that this tool is superior to classical EAE scoring methods in detecting early motor deficits and assessing disease severity.

Compared to the other two MS models, the application of automated tracking in TMEV-IDD has been uncommon. The spontaneous box (Digiscan activity monitoring system) has been used by McGavern et al.

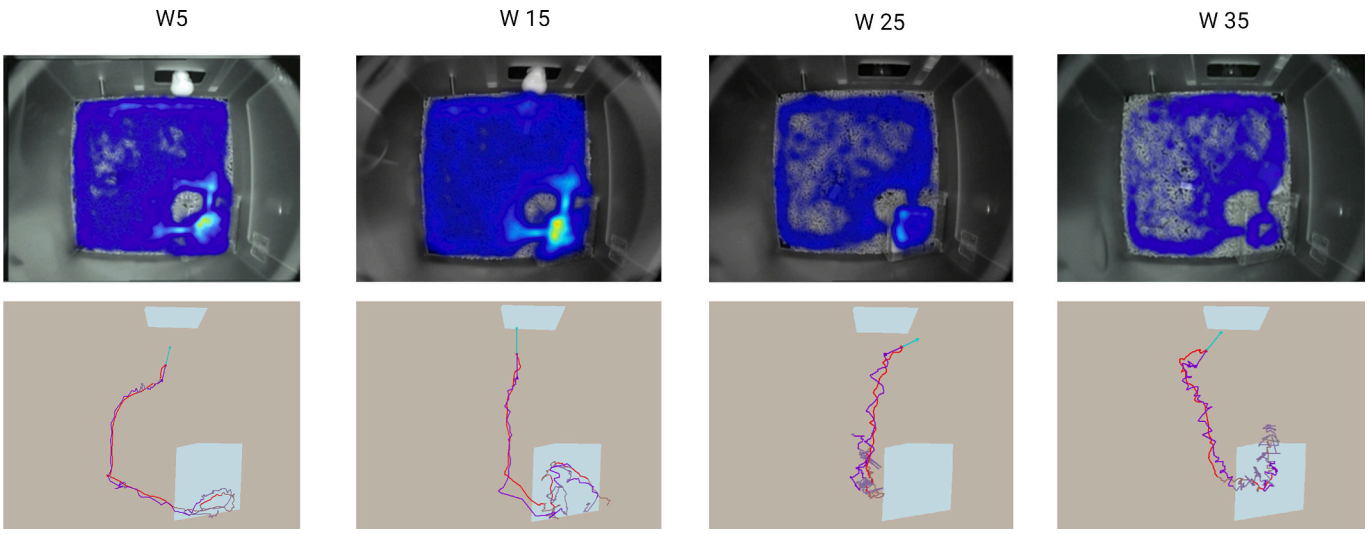

Fig. 7. Above: Heatmaps of walking frequency (22h) at different time points post-infection in one ^{v}SJL-infected mouse.
Below: The trajectory from the shelter to the feeder (last 15 s) for the center point (red line) and tail-base point (purple line) of the same mouse at different time points post-infection. (For interpretation of the references to colour in this figure legend, the reader is referred to the web version of this article.)

(1999) together with nonautomated methods to quantify motor deficits. They assessed different strains of mice, including SJL, at two time points post-infection and followed their nocturnal spontaneous activity. More recently, Mestre et al. (2021) employed the same system (Digiscan Analyzer) to measure spontaneous locomotion in ^{v}SJL and ^{m}SJL mice from week 10 to week 40 pi, in 10-min-long sessions. Our setup used the combination of PhenoTyper cages and Ethovision software (Noldus IT) to track the same individual, for 22 h every 2 weeks and over 37 weeks after TMEV inoculation.

Table 2 below compares the different protocols using automated measurement of spontaneous locomotion in TMEV-IDD.

In both studies, it was reported that spontaneous locomotion decreased in ^{v}SJL mice compared to mock-infected mice in the period between week 10 and week 12 post-infection. This early decline in spontaneous activity did not match our findings at week 13 for distance covered, frequency of walking and frequency of rearing. Nevertheless, we did notice a drop in velocity compared to baseline in ^{v}SJL but not in ^{m}SJL mice. Moreover, there was a significant difference between them in rearing, but not in walking velocity. Whether these contrasting results are due to sample size, individual variations, the data acquisition method, length of trials or something else is difficult to say.

Our findings regarding walking and rearing frequency were in line with those from the longitudinal follow-up in Mestre et al. (2021), who also noted a decrease in spontaneous locomotion in aged ^{m}SJL mice. They attributed this to both age-related neurodegenerative changes in older mice, as well as lack of novelty after repeated recordings in the same environment.

The decrease in these parameters in ^{v}SJL mice was indicative of TMEV-related motor deficits; however, it was difficult to determine from those data alone to what extent the virus contributed to those deficits. Strikingly, the SJL strain has been used as a prototype TMEV strain for many years, yet there are very few reports on declining spontaneous activity in healthy individuals obtained with traditional measurement methods. McGavern et al. (1999) did, however, observe that both age and intracerebral injection could influence rotarod performance.

While our findings align with those of Mestre et al. regarding walking and rearing frequency, we identified an additional spontaneous locomotion parameter that proved to be key in distinguishing age-related from TMEV-related deficits in this strain. The velocity during both horizontal and vertical movement did not decline in ^{m}SJL mice as opposed to ^{v}SJL mice, further confirming the sensitivity of the video tracking system. The decrease in this parameter could be attributed to

Table 2
Comparison of our methodology and results on spontaneous locomotion with two other similar studies using the SJL strain.

Study	McGavern et al., 1999	Mestre et al., 2021	This study, 2023
Method and system	Digiscan activity monitoring system	Activity cage + Digiscan Analyzer (Activity Monitor System; Omnitech Electronics Inc.)	Phenotyper cages plus Ethovision 16 (Noldus IT)
Number of mice	6 mock/6 TMEV 3 of each per box – repeated twice	11 mock/15 TMEV for longitudinal study (+7 of each for week 12 tracking)	12 mock/12 TMEV for longitudinal study
Frequency of data acquisition	Two time ranges 55–71 days pi and 98–128 days pi	Once a week from week 10 to week 40 pi	Every second week for 37 weeks pi
Duration of data acquisition per recording session	80 consecutive hours (only nocturnal activity analyzed)	10 min	22 h
Total acquisition duration (per mouse)	80 h	5 h	418 h
Parameters measured	Horizontal and vertical activity Hourly infrared beam interruptions from 6 PM to 5 AM over the 3-day analysis period	Horizontal and vertical activity Total number of horizontal and vertical sensor beam interruptions (ambulatory units)	Horizontal and vertical activity Total frequency of walking and rearing, distance covered during walking (cm) and velocity of the center point during walking and rearing (cm/s)
Time of significant differences between ^{v}SJL and ^{m}SJL mice	55 to 71 days pi (week 8 -week 10) and 98 to 128 days pi (week 14 - week 18)	Week 12 pi Week 18 pi Week 24 pi	After week 27 pi
Declining trend in activity in both ^{v}SJL and ^{m}SJL mice	Not mentioned	Yes, for both horizontal and vertical activity	Yes, for walking, distance covered and rearing No for velocity

the loss of large and medium myelinated axons during the late progressive phase of TMEV (dpi 195–220, or weeks 27–31 pi) that has been described in ^{v}SJL mice (McGavern et al., 2000a, 2000b) and results in severe spinal cord atrophy and functional impairments. The same study demonstrated reduced conduction velocity in the axons of affected SJL mice – this could clinically manifest as reduced velocity of movement. Interestingly, ^{v}SWR mice did not display a severe decline in velocity, which might indicate that they do not suffer the same degree of axonal loss.

Our study demonstrates that changes in spontaneous locomotion become markedly apparent only after longitudinal follow-up of the same group of individuals over an extended period. A potential caveat of short-term measurements with limited duration is failure to notice the influence that external and internal factors have on the obtained results. While those methods might be suitable for use in other, shorter, MS models (cuprizone and EAE), the TMEV-IDD model is lengthy and covers almost an entire mouse lifespan. The use of long-term automated tracking for 22 h allowed us to gain better insight into the variables that affect spontaneous locomotion in TMEV-infected and in mock-infected mice. Furthermore, by measuring multiple parameters, we identified the velocity of the center point as a parameter that is not significantly influenced by age, motivation or habituation, and is thus suitable for the quantification of motor deficits in this model.

The frequency of data collection might also influence the interpretation of results. Many TMEV studies are designed to "snapshot" data at intervals of 3, 6 and 9 months. While that might be more practical and convenient, it may overlook some of the effects of the virus on locomotion and behavior. We therefore decided to collect individual data every two weeks to assess TMEV's progression.

In addition to changes in spontaneous locomotion, gait alteration, especially a waddling gait, is the hallmark clinical sign of TMEV-induced demyelinating disease (Dal Canto and Lipton, 1977). This "wobbly" gait is clearly observable in infected mice; however, the matter of quantifying it is not as straightforward. The footprint analysis test has been used with great success to characterize primary locomotor gait and has been performed in TMEV-IDD (Brinkmeyer-Langford et al., 2017; McGavern et al., 1999) to assess the progression of neurologic deficits. Recently, specialized automated tools for gait assessment have been developed, e.g., DigiGait, which has been used in the TMEV model (Brinkmeyer-Langford et al., 2017; Karmakar et al., 2023) and CatWalk XT (Noluds IT), which has been used in other neurodegenerative disease models (Timotius et al., 2023; Walter et al., 2022; Zhu et al., 2023).

While these tools are extremely valuable for detailed gait assessment, handling the mice immediately prior to the test might cause stress, there are duration constraints and gait is not evaluated during spontaneously occurring locomotion.

In contrast, our method allows us to detect TMEV-related gait alterations simultaneously to changes in spontaneous locomotion and behavior, using a single data-collection tool. Furthermore, it evaluates the walking gait of freely moving TMEV-infected mice for a duration of 22 h as opposed to a single predetermined time point, increasing the reproducibility of the results. Finally, we can visualize the progression of the disease using the path trajectory of mice as well as the video footage, thus confirming the data output.

McGavern et al. (1999) reported gait alterations in ^{v}SJL mice at dpi 94 (week 13) by measuring forelimb and hind limb length of stride. As mentioned above, this coincides with the peak demyelinating phase of early TMEV-IDD. This result is in agreement with ours from recording week 13 pi (dpi 97), when ^{v}SJL mice displayed statistically significant differences from baseline for all three parameters quantifying gait alterations. In another study, McGavern et al. (2000a, 2000b) described gait alterations in the form of reduced hindlimb width during the late, chronic stage of TMEV-IDD (dpi 171, dpi 184). Again, this coincides with our findings of a wobbly gait in the later stages of chronic TMEV-IDD in ^{v}SJL, although we observed these changes slightly later (dpi 195–265). Notably, no gait alterations were observed in ^{m}SJL mice at any time point.

We also compared the TMEV-IDD course in two susceptible strains of mice: SJL/J and SWR. In TMEV studies, SJL has mostly been compared to the resistant C57BL/6 strain (Oleszak et al., 2004), as well as other susceptible strains like B10Q and FVB (Bieber et al., 2005). Genetically, these two strains are very similar, but they differ in haplotype at the major histocompatibility complex (MHC H-2 locus), with SJL having an H-2 s haplotype while SWR has an H-2q haplotype (Lindahl, 1997). What is known about the two strains in the context of TMEV infection is that while both strains are susceptible to virus-induced demyelination, there are key differences in their responses during the late chronic stages of the disease. Histological studies have demonstrated that the two strains differ in their capacity for myelin repair after TMEV infection (Bieber et al., 2005).

In SJL, the progressive motor decline that accompanies the final stages of the disease has been well documented. In SWR, however, little is known about the clinical manifestation of the disease, apart from gait alterations in the first few months (Nicholson et al., 1995). Bieber (2005) also reported that SWR's rotarod performance during TMEV-IDD is not as affected as SJL's. Because of its known hyperexcitability, the lack of data on this strain's motor capability may reflect difficulties associated with traditional measurement methods. With our approach, we were able to measure SWR's performance in a noninvasive way, thus eliminating such issues.

We demonstrated that the two strains displayed distinct patterns of TMEV-IDD evolution. SJL, as a prototype TMEV-susceptible strain, suffers earlier and more severe decline in spontaneous locomotion, but both strains suffer significant gait deficits. This is in line with the data that describe gait alterations as one of the main hallmarks of TMEV. Our results reveal that this TMEV-specific clinical sign can be reliably measured via video tracking technology.

Spontaneous horizontal and vertical locomotion were reduced in both strains as the disease progressed, but earlier deficits were apparent in the SJL strain. Once again, velocity during horizontal and vertical movements emerged as a key parameter by which to highlight differences between the strains, with a dramatic decrease in SJLs, as opposed to SWRs. Retrograde neuronal labeling (Bieber et al., 2005) showed that axonal injury after TMEV infection was less pronounced in SWR compared to SJL mice, which could explain their preserved motor function.

Gait deficits followed different patterns in both strains: they appeared later and were more progressive in SWR compared to an intermittent appearance in SJL. This could reflect different host–virus dynamics in the two strains.

Our data also put in perspective other interesting findings regarding the timing of demyelination and axonal loss following TMEV infection. According to McGavern et al. (2000a, 2000b), demyelination progressively increases up to 100 dpi; however, this is not accompanied by a significant loss of myelinated fibers. This results in early electrophysiological alterations around 45 to 90 dpi. During the late chronic TMEV phase (190–220 dpi) the significant loss of fast conducting large fibers leads to severe neurological deficits. Our results are in support of this: gait alterations were first visible in ^{v}SJL mice at week 13 (dpi 97), matching the peak of demyelination. Mice also showed transient drop in velocity at the same time point; however, their overall spontaneous activity was not affected. It was only after week 27 (dpi 195) that these mice showed a progressive decrease in their spontaneous locomotion. On the other hand, ^{v}SWR mice demonstrated significant gait alterations starting from week 21 (dpi 143) onwards, but without a significant decline in their spontaneous locomotion levels. An assumption might be made from all this that gait impairments are a direct consequence of demyelination events, while progressive loss of motor function (measured via a decline in spontaneous locomotion) is the result of axonal degeneration beyond repair. Obviously, both strains suffer from virus-induced demyelination, but they seem to differ in the degree of axonal loss. Further experiments to assess axonal integrity in these

strains, such as immunohistochemistry and/or measurement of associated biomarkers, could solidify these observations and offer insight into the mechanisms behind the differences.

We have also described (to our knowledge for the first time) how maintenance and exploratory behaviors are influenced by TMEV infection. Maintenance behaviors such as grooming and eating did not change significantly throughout the nine months post-infection, suggesting that the general wellbeing of the animals was preserved.

Exploratory behavior decreased in both ^{v}SJL and ^{v}SWR and in ^{m}SJL. This may be due to age-related cognitive deficits, habituation and/or TMEV-induced neuronal degeneration. While active exploration was expected to decrease after multiple exposures to the same recording environment, that was not the case for ^{m}SWR mice, which suggests hyperactivity in healthy mice from this strain.

Moreover, in addition to TMEV-related outcomes, by employing this manner of phenotyping, we observed interesting findings in the control mice of both strains. The decrease in activity in ^{m}SJL mice due to aging/lack of novelty in the recording environment that we (and others) have observed, highlights other factors that can significantly influence the results in long-term behavioral studies. On the other hand, the progressive increase in activity in ^{m}SWR mice might implicate emotional reactivity to a novel environment after a repeated procedure in this strain.

Lastly, some of the parameters we measured resemble those used to assess disability in patients with MS (Abbadessa et al., 2021; Bradshaw et al., 2017), which showcases the potential translational value of our study.

7. Conclusions

We have demonstrated that the described automated video tracking method can be reliably employed for the quantification of TMEV-IDD progression in different mouse strains. Our phenotyping results are in line with other reports on differences in the axonal pathology between the SJL and SWR strains following TMEV-IDD induction.

Moreover, we have shown that the system is sensitive enough to discriminate between age- and virus-related deficits in mock-infected and infected mice from the same strains. The parameters that we have described were derived from data obtained in a noninvasive manner and might be useful for the future assessment of TMEV-induced phenotypes, as well as for testing the efficacy of new treatment compounds for progressive multiple sclerosis.

Supplementary data to this article can be found online at https://doi.org/10.1016/j.expneurol.2024.114851.

Funding

This research was funded by Laboratoires Prevor, Moulin de Verville, 95760 Valmondois, France.

Ethics approval

The study was approved by the University of Liege Ethics Committee (Approval Number 20–2229).

CRediT authorship contribution statement

Iskra Djabirska: Writing – review & editing, Writing – original draft, Visualization, Validation, Methodology, Investigation, Formal analysis, Data curation, Conceptualization. **Laetitia Delaval:** Investigation. **Audrey Tromme:** Investigation. **Joël Blomet:** Funding acquisition. **Daniel Desmecht:** Writing – review & editing, Validation, Supervision, Project administration, Methodology, Conceptualization. **Anne-Sophie Van Laere:** Writing – review & editing, Validation, Supervision, Methodology, Investigation, Formal analysis, Conceptualization.

Declaration of competing interest

The authors declare the following financial interests/personal relationships which may be considered as potential competing interests:

Djabirska Iskra, Delaval Laetitia, Tromme Audrey, Van Laere Anne-Sophie reports financial support was provided by Prevor Research Laboratories. If there are other authors, they declare that they have no known competing financial interests or personal relationships that could have appeared to influence the work reported in this paper.

Data availability

Data will be made available on request.

Acknowledgements

The authors wish to thank Prof. Frédéric Farnir for valuable discussions.

The graphical abstract was created using Biorender.com.

References

Abbadessa, G., Lavorgna, L., Miele, G., Mignone, A., Signoriello, E., Lus, G., Clerico, M., Sparaco, M., Bonavita, S., 2021. Assessment of multiple sclerosis disability progression using a wearable biosensor: A pilot study. J. Clin. Med. 10 (6) https://doi.org/10.3390/jcm10061160.

Bass, J.S., Tuo, A.H., Ton, L.T., Jankovic, M.J., Kapadia, P.K., Schirmer, C., Krishnan, V., 2020. On the digital psychopharmacology of valproic acid in mice. Front. Neurosci. 14 https://doi.org/10.3389/fnins.2020.594612.

Bieber, A.J., Ure, D.R., Rodriguez, M., 2005. Genetically dominant spinal cord repair in a murine model of chronic progressive multiple sclerosis. J. Neuropathol. Exp. Neurol. 64 (1), 46–57. https://doi.org/10.1093/jnen/64.1.46.

Bradshaw, Michael J., Farrow, Samantha, Motl, Robert W., Chitnis, Tanuja, 2017. Wearable biosensors to monitor disability in multiple sclerosis. Neurology 7 (4), 354–362. http://www.embase.com/search/results?subaction=viewrecord&from=export&id=L617843638%0Adoi:10.1212/CPJ.0000000000000382.

Brinkmeyer-Langford, C.L., Rech, R., Amstalden, K., Kochan, K.J., Hillhouse, A.E., Young, C., Welsh, C.J., Threadgill, D.W., 2017. Host genetic background influences diverse neurological responses to viral infection in mice. Sci. Rep. 7 (1), 1–17. https://doi.org/10.1038/s41598-017-12477-2.

Brooks, S.P., Dunnett, S.B., 2009. Tests to assess motor phenotype in mice: A user's guide. Nat. Rev. Neurosci. 10 (7) https://doi.org/10.1038/nrn2652.

Buddeberg, B.S., Kerschensteiner, M., Merkler, D., Stadelmann, C., Schwab, M.E., 2004. Behavioral testing strategies in a localized animal model of multiple sclerosis. J. Neuroimmunol. 153 (1–2) https://doi.org/10.1016/j.jneuroim.2004.05.006.

Cisbani, G., Poggini, S., Laflamme, N., Pons, V., Tremblay, M.È., Branchi, I., Rivest, S., 2021. The Intellicage system provides a reproducible and standardized method to assess behavioral changes in cuprizone-induced demyelination mouse model. Behav. Brain Res. 400 https://doi.org/10.1016/j.bbr.2020.113039.

Crawley, J.N., 2003. Behavioral phenotyping of rodents. Compar. Med. 53 (2).

Dal Canto, M.C., Lipton, H.L., 1977. Multiple sclerosis. Animal model: Theiler's virus infection in mice. Am. J. Pathol. 88 (2).

Denic, A., Johnson, A.J., Bieber, A.J., Warrington, A.E., Rodriguez, M., Pirko, I., 2011. The relevance of animal models in multiple sclerosis research. Pathophysiology 18 (1). https://doi.org/10.1016/j.pathophys.2010.04.004.

Dumont, M., 2011. Behavioral phenotyping of mouse models of neurodegeneration. Methods Mol. Biol. 793 https://doi.org/10.1007/978-1-61779-328-8_15.

Eldridge, R., Osorio, D., Amstalden, K., Edwards, C., Young, C.R., Cai, J.J., Konganti, K., Hillhouse, A., Threadgill, D.W., Welsh, C.J., Brinkmeyer-Langford, C., 2020. Antecedent presentation of neurological phenotypes in the collaborative cross reveals four classes with complex sex-dependencies. Sci. Rep. 10 (1) https://doi.org/10.1038/s41598-020-64862-z.

Gilli, F., Royce, D.B., Pachner, A.R., 2016. Measuring progressive neurological disability in a mouse model of multiple sclerosis. J. Vis. Exp. 2016 (117) https://doi.org/10.3791/54616.

Grieco, F., Bernstein, B.J., Biemans, B., Bikovski, L., Burnett, C.J., Cushman, J.D., van Dam, E.A., Fry, S.A., Richmond-Hacham, B., Homberg, J.R., Kas, M.J.H., Kessels, H.W., Koopmans, B., Krashes, M.J., Krishnan, V., Logan, S., Loos, M., McCann, K.E., Parduzi, Q., Noldus, L.P.J.J., 2021. Measuring behavior in the home cage: study design, applications, challenges, and perspectives. Front. Behav. Neurosci. 15 https://doi.org/10.3389/fnbeh.2021.735387.

Haynell, A., Marklund, N., 2014. Structured evaluation of rodent behavioral tests used in drug discovery research. Front. Behav. Neurosci. 8, 252. https://doi.org/10.3389/fnbeh.2014.00252.

Johnson, R.R., Prentice, T.W., Bridegam, P., Young, C.R., Steelman, A.J., Welsh, T.H., Welsh, C.J.R., Meagher, M.W., 2006. Social stress alters the severity and onset of the chronic phase of Theiler's virus infection. J. Neuroimmunol. 175 (1–2) https://doi.org/10.1016/j.jneuroim.2006.02.014.

Karmakar, M., Pérez Gómez, A.A., Carroll, R.J., Lawley, K.S., Amstalden, K.A.Z., Welsh, C.J., Threadgill, D.W., Brinkmeyer-Langford, C., 2023. Baseline gait and motor function predict long-term severity of neurological outcomes of viral infection. Int. J. Mol. Sci. 24 (3) https://doi.org/10.3390/ijms24032843.

Kingwell, E., Marriott, J.J., Jetté, N., Pringsheim, T., Makhani, N., Morrow, S.A., Fisk, J. D., Evans, C., Béland, S.G., Kulaga, S., Dykeman, J., Wolfson, C., Koch, M.W., Marrie, R.A., 2013. Incidence and prevalence of multiple sclerosis in Europe: A systematic review. BMC Neurol. 13 https://doi.org/10.1186/1471-2377-13-128.

Lindahl, K.F., 1997. On naming H2 haplotypes: functional significance of MHC class Ib alleles. Immunogenetics 46 (1). https://doi.org/10.1007/s002510050242.

McGavern, D.B., Zoecklein, L., Drescher, K.M., Rodriguez, M., 1999. Quantitative assessment of neurologic deficits in a chronic progressive murine model of CNS demyelination. Exp. Neurol. 158 (1) https://doi.org/10.1006/exnr.1999.7082.

McGavern, D.B., Murray, P.D., Rivera-Quiñones, C., Schmelzer, J.D., Low, P.A., Rodriguez, M., 2000a. Axonal loss results in spinal cord atrophy, electrophysiological abnormalities and neurological deficits following demyelination in a chronic inflammatory model of multiple sclerosis. Brain 123 (3). https://doi.org/10.1093/brain/123.3.519.

McGavern, D.B., Zoecklein, L., Sathornsumetee, S., Rodriguez, M., 2000b. Assessment of hindlimb gait as a powerful indicator of axonal loss in a murine model of progressive CNS demyelination. Brain Res. 877 (2) https://doi.org/10.1016/S0006-8993(00)02710-4.

Mestre, L., Alonso, G., Feliú, A., Mecha, M., Martín, C., Villar, L.M., Guaza, C., 2021. Aging and neuroinflammation: changes in immune cell responses, axon integrity, and motor function in a viral model of progressive multiple sclerosis. Aging Cell 20 (9). https://doi.org/10.1111/acel.13440.

Milo, R., Kahana, E., 2010. Multiple sclerosis: Geoepidemiology, genetics and the environment. Autoimmun. Rev. 9 (5) https://doi.org/10.1016/j.autrev.2009.11.010.

Nicholson, S.M., Jokinen, D.M., Dal Canto, M.C., Kim, B.S., Melvold, R.W., 1995. Genetic analysis of susceptibility to Theiler's murine encephalomyelitis virus-induced demyelinating disease in the SWR strain. J. Neuroimmunol. 59 (1–2) https://doi.org/10.1016/0165-5728(95)00020-3.

Oleszak, E.L., Chang, J.R., Friedman, H., Katsetos, C.D., Platsoucas, C.D., 2004. Theiler's virus infection: A model for multiple sclerosis. Clin. Microbiol. Rev. 17 (1), 174–207. https://doi.org/10.1128/CMR.17.1.174-207.2004.

Palumbo, S., Pellegrini, S., 2017. Experimental in vivo models of multiple sclerosis: state of the art. In: Multiple Sclerosis: Perspectives in Treatment and Pathogenesis. https://doi.org/10.15586/codon.multiplesclerosis.2017.ch11.

Patrikios, P., Stadelmann, C., Kutzelnigg, A., Rauschka, H., Schmidbauer, M., Laursen, H., Sorensen, P.S., Brück, W., Lucchinetti, C., Lassmann, H., 2006. Remyelination is extensive in a subset of multiple sclerosis patients. Brain 129 (12). https://doi.org/10.1093/brain/awl217.

Paz Soldán, M.M., Raman, M.R., Gamez, J.D., Lohrey, A.K., Chen, Y., Pirko, I., Johnson, A.J., 2015. Correlation of brain atrophy, disability, and spinal cord atrophy in a murine model of multiple sclerosis. J. Neuroimaging 25 (4). https://doi.org/10.1111/jon.12250.

Procaccini, C., De Rosa, V., Pucino, V., Formisano, L., Matarese, G., 2015. Animal models of multiple sclerosis. Eur. J. Pharmacol. 759, 182–191. Elsevier B.V. https://doi.org/10.1016/j.ejphar.2015.03.042.

Richardson, C.A., 2015. The power of automated behavioural homecage technologies in characterizing disease progression in laboratory mice: A review. Appl. Anim. Behav. Sci. https://doi.org/10.1016/j.applanim.2014.11.018.

Robinson, L., Riedel, G., 2014. Comparison of automated home-cage monitoring systems: emphasis on feeding behaviour, activity and spatial learning following pharmacological interventions. J. Neurosci. Methods. https://doi.org/10.1016/j.jneumeth.2014.06.013.

Shahi, S.K., Freedman, S.N., Dahl, R.A., Karandikar, N.J., Mangalam, A.K., 2019. Scoring disease in an animal model of multiple sclerosis using a novel infrared-based automated activity-monitoring system. Sci. Rep. 9 (1) https://doi.org/10.1038/s41598-019-55713-7.

Sheridan, G.K., Dev, K.K., 2014. Targeting S1P receptors in experimental autoimmune encephalomyelitis in mice improves early deficits in locomotor activity and increases ultrasonic vocalisations. Sci. Rep. 4 https://doi.org/10.1038/srep05051.

Timotius, I.K., Roelofs, R.F., Richmond-Hacham, B., Noldus, L.P.J.J., von Hörsten, S., Bikovski, L., 2023. CatWalk XT gait parameters: a review of reported parameters in pre-clinical studies of multiple central nervous system and peripheral nervous system disease models. Front. Behav. Neurosci. 17 https://doi.org/10.3389/fnbeh.2023.1147784.

Tsunoda, I., Fujinami, R.S., 2010. Neuropathogenesis of theiler's murine encephalomyelitis virus infection, an animal model for multiple sclerosis. J. NeuroImmune Pharmacol. 5 (3), 355–369. https://doi.org/10.1007/s11481-009-9179-x.

Voikar, V., Gaburro, S., 2020. Three pillars of automated home-cage phenotyping of mice: novel findings, refinement, and reproducibility based on literature and experience. Front. Behav. Neurosci. 14 https://doi.org/10.3389/fnbeh.2020.575434.

Walter, J., Mende, J., Hutagalung, S., Grutza, M., Younsi, A., Zheng, G., Unterberg, A.W., Zweckberger, K., 2022. Focal lesion size poorly correlates with motor function after experimental traumatic brain injury in mice. PLoS One 17 (3 March). https://doi.org/10.1371/journal.pone.0265448.

Zhu, Q., Song, J., Chen, J.Y., Yuan, Z., Liu, L., Xie, L.M., Liao, Q., Ye, R.D., Chen, X., Yan, Y., Tan, J., Heng Tan, C.S., Li, M., Lu, J.H., 2023. Corynoxine B targets at HMGB1/2 to enhance autophagy for α-synuclein clearance in fly and rodent models of Parkinson's disease. Acta Pharm. Sin. B. https://doi.org/10.1016/j.apsb.2023.03.011.

Web references

https://mousebehavior.org/active-behavior/.
https://mousebehavior.org/maintenance-behavior.